ISSN 1392–124X (print), ISSN 2335–884X (online) INFORMATION TECHNOLOGY AND CONTROL, 2014, T. 43, Nr. 3

A Powerful yet Efficient Iris Recognition Based on Local Binary Quantization

Raed T. Al-Zubi

Electrical Engineering Department, The University of Jordan
Amman 11942, Jordan
e-mail: r.alzubi@ju.edu.jo

Khalid A. Darabkh

Computer Engineering Department, The University of Jordan
Amman 11942, Jordan
e-mail: k.darabkeh@ju.edu.jo

Yaser I. Jararweh

Computer Science Department, Jordan University of Science and Technology
Irbid 22110, Jordan
e-mail: yijararweh@just.edu.jo

crossref http://dx.doi.org/10.5755/j01.itc.43.3.5225

Abstract. A secure identification system based on human iris recognition has been an attractive goal for researchers for a long time. In this paper, we propose an efficient iris recognition scheme. To significantly reduce the computational time that is required for locating the iris boundaries in a captured eye image, only the 3- and 9- o'clock sides of the iris are considered in our scheme as a search area for finding the outer boundary of the iris. The donut-shape of the iris is then mapped into a rectangular region with constant dimensions to mitigate the problem of changing the iris size that may occur due to having variations in the image capturing conditions. Thenceforth, the lower half of the iris ring is considered as a region of interest for feature extraction. This region is slightly interfered by eyelids and eyelashes. The feature extraction process is performed by a proposed *local binary quantization* technique. This technique requires a lower computational time than that of other techniques that extract the features of an iris using wavelet analysis (i.e., such as Fourier and Gabor analysis). It should be borne in mind that the computational time of wavelet analysis could be a challenge in online applications. Furthermore, the parameters of wavelet analysis are set in advance and hence they may not adapt with some noises and changes in the iris image as a result of having variations in the image capturing conditions. However, the proposed *local binary quantization* technique is not affected by these variations. The CASIA iris database is used to conduct several experiments that show the performance of the proposed scheme. Compared to other schemes, the proposed scheme achieves a correct segmentation rate of 99% at a low segmentation time and a correct recognition rate of 99.34%.

Keywords: Iris Recognition; local binary quantization; feature extraction.

1. Introduction

A secure personal identification system is one of the vital necessities in these days. Designing such a system based on the human iris (see Fig. 1) was found to be a solution that satisfies the required degree of security [1–6]. The human iris has important features that support it to be a suitable choice for a secure personal identification system; the human iris has a distinctive and stable (during life) spatial pattern (not as face recognition [7]) where it can be remotely captured. Several systems were proposed for capturing iris image [1, 2, 5, 8–11]. The captured iris image is then passed through four-steps process (see Fig. 2): iris segmentation (i.e., finding the region of the iris in an eye image), iris normalization (i.e., mapping the textural details of the iris ring into a fixed-size matrix to account for the possible differences in the size of irises during image capturing process), feature extraction (i.e., recording the textural details of the iris in a feature vector), as well as features matching (i.e., calculating the similarity degree between the compared feature vectors).

A practical iris-based recognition system could be used as a large scale identification system with possibly millions of people. Hence, designing iris recognition scheme is not so simple. An iris recognition scheme should be fast and accurate. Most of the well known schemes that were proposed for iris recognition are based on applying the Hough transform over the entire eye image to locate the iris boundaries and using wavelet analysis for feature extraction [13]. The main drawback of these techniques is its huge computational time [14–17]. Moreover, the input parameters of the wavelet analysis are selected and fixed in advance [13], hence these parameters may be unsuitable for different image capturing conditions (i.e., different capturing distance, different light intensity, etc.). Unlike these schemes, our proposed scheme is fast and adaptive for image capturing conditions. In other words, to substantially reduce the computational time that is required for iris segmentation, our proposed scheme searches for the outer boundary within a small (instead of the entire image) yet useful regions (i.e., the 3- and 9 o'clock sides of the iris). Next to that, the segmented iris region is mapped into a fixed-size matrix. Afterwards, discriminating features from the iris are extracted by mapping the gray-value of each point in the normalized iris into one binary levels: 0 or 1. These levels are generated via binary quantization of the intensity changes within a certain neighborhood of the mapped point. Compared with the traditional feature extraction methods that are based on wavelet analysis, the proposed approach is simple and has low computational time as well as it is auto-adaptive with possible changes in image capturing conditions. It can not be missed out to be mentioned that the degree of similarity between different irises is measured by calculating the Hamming distance between the feature vectors of these irises. Several experiments are conducted using CASIA database to evaluate the performance of the proposed scheme in verification and identification modes.

The structure of the rest of the paper is as follows: we provide the related work in Section 2. In Section 3, we discuss the proposed scheme for iris recognition. In Section 4, different experiments are conducted using CASIA iris database [12] to evaluate and compare the performance of the proposed scheme with other well-known schemes. In Section 5, we provide the conclusions.

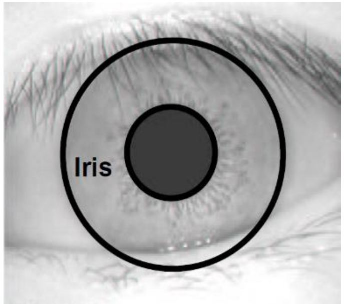

Figure 1. A human iris image (i.e., image 014-2-2 from CASIA database [12])

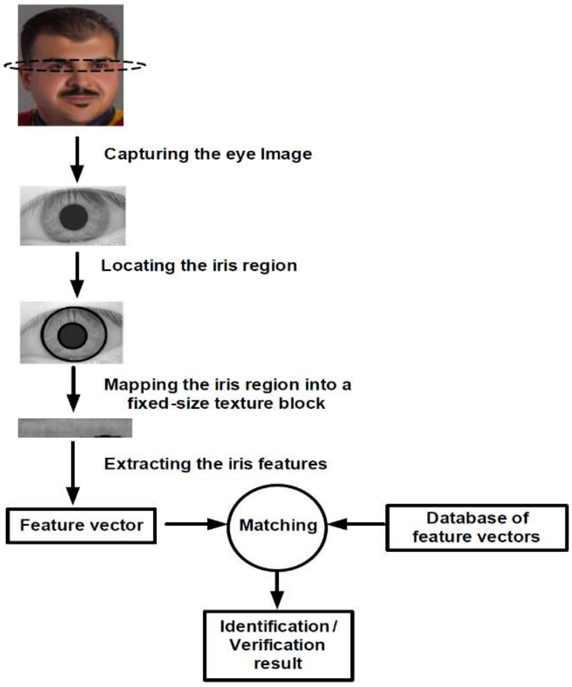

Figure 2. Steps of iris recognition system

2. Related Work

Different algorithms have been suggested for iris recognition (see [2], [18], [19], [20], [5], [21], [22], [10], [23], [24], [25], [26], [27], [28], [29], [30], [31], [32], [33], [34], [35], [36], [13]). In this section, we present the ones that are relevant and comparable with our proposed algorithm. The iris recognition algorithm proposed in [2] [18], [19], [20] is known as a reference for almost all new proposed algorithms. In this algorithm, a certain integro-differential function was employed for iris segmentation. Then, the iris region was mapped into a fixed-size matrix. After that, 2D Gabor functions were used to extract the textural features from the iris region and encode these features into a 2048-bit code. Finally, these codes were compared by calculating the Hamming distance between them. Wildes et al. [5] located the iris ring in an eye image by employing the edge detection technique and Hough transform. Then, a Laplacian of Gaussian function was used to filter the iris region and represent the textural information of the iris. Finally, the matching was done by using a normalized correlation technique. In [21], the feature extraction process was performed using different levels of 1D wavelet applied over different circles centralized over the iris ring. Two specific functions were used to calculate the dissimilarity between the compared irises. In [24], multi-channel Gabor functions were used to extract detailed textural information from the iris region. Then, a weighted Euclidean distance was calculated for iris comparisons. In [25], circular symmetric filters were employed for extracting the textural details of the iris region. For the iris matching, a nearest feature line technique was used. In [27], a group of filters with different parameters were used to construct a feature vector. Then, the size of the feature vector was reduced by using Fisher linear discriminant. Finally, the nearest center classification was employed for the iris matching process. In [26], for iris segmentation, several image processing techniques were used: canny edge detection, circular and linear Hough transform (Radon transform), simple thresholding technique. For feature extraction, a log-Gabor filter was used. In [31], the inner and outer boundaries of the iris were located by adopting the edge detection technique and Hough transform. Then, a polynomial fitting technique was used to locate the upper and lower eyelids. To extract the angular iris information, a 1D log-Gabor filter was adopted. In [32], a dual tree complex wavelet was applied for feature extraction. In [33], the authors applied four-level wavelet transformation to get a binary feature vector. In [34], a group of high frequency coefficients for two dimensional complex wavelet transformation was used as discriminating features of the iris region. In [36], an efficient eyelids segmentation method was suggested and a Haar wavelet transformation was adopted to extract iris features.

In this paper, an efficient iris recognition scheme is proposed. We intend in this work to propose a fast and accurate recognition scheme. The scheme is mainly based on analyzing the texture of the iris image by using local binary quantization.

3. Proposed Scheme for Iris Recognition

In this section, we discuss our proposed iris recognition scheme. The main steps of the proposed scheme (see Fig. 2) are: iris segmentation, iris normalization, feature extraction, and matching.

3.1. Iris Segmentation

As shown in Fig. 1, the iris region is bounded by two boundaries: the inner one which is determined by the pupil region and the outer one which is determined by the sclera. These boundaries can be considered as two concentric circles [2, 5, 9, 10, 22–25, 27]. As suggested in [31], in our proposed scheme, we consider the fact that the inner boundary can be most likely approximated as an ellipse [6].

The steps of the proposed algorithm for iris segmentation are illustrated as follows:

- **Locating the inner boundary:** we follow the same method used in [31] to locate the iris inner boundary. In this method, edge detection technique is used, then elliptical Hough transform is applied to locate the inner boundary. Fig. 3 shows the result of this step.

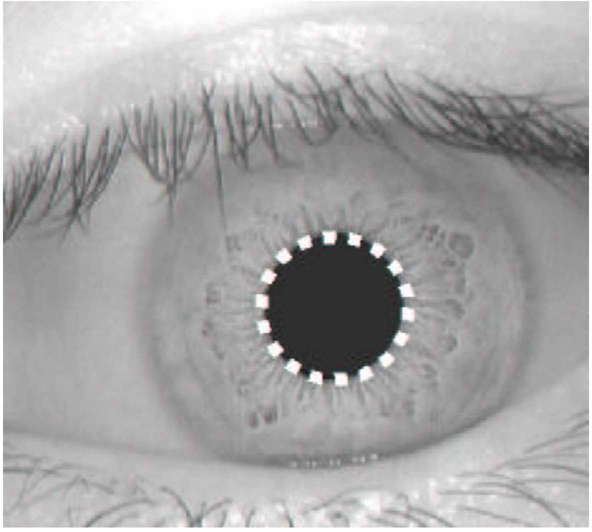

Figure 3. Finding the inner boundary of the iris in image 027-2-7 from CASIA database [12]

- **Locating the outer boundary:** in this step, the proposed scheme is based on the fact that the 3-o'clock and 9-o'clock sides of the outer boundary of an iris are usually the most clear parts of the boundary (i.e., slightly interfered by eyelashes or eyelids), see Fig. 4(a). Beside this fact, the proposed scheme exploits the result that the ratio of the pupil radius to the iris radius is in the range of 0:25 to 0:60 [31]. Accordingly, the proposed scheme determines the search regions to find the outer boundary, see Fig. 4(a). Thereafter, to locate the boundary, these 3-o'clock and 9-o'clock regions are filtered by east and west compass kernels, respectively, see Fig. 4(b). After that, the filtered regions are converted to binary regions (see Fig. 4(c)) in order to apply the circular Hough transform to find the outer boundary, see Fig. 4(d). To consider the fact that the inner and outer iris boundaries are not always cocentric, the applied Hough transform searches for the center of the outer boundary within a small margin (±5 pixels) around the center of the inner boundary. It is clear that applying the Hough transform within a certain regions (i.e., 3-o'clock and 9-o'clock regions) will reduce the computational time, which is the main issue of using Hough transform in online applications.

3.2. Iris Normalization

Image capturing conditions (i.e., capturing distance, light intensity, etc.) may vary, which result in having changes in the size of the captured iris image. Therefore, we use Daugman's normalization method [4] (see Fig. 5) to map the iris region into a predetermined-size matrix. In [26] and [31], the authors proved that the proper size for this matrix is 20x240 elements. According to the Daugman's normalization method, each point in the iris ring (i.e., located in cartesian coordinates (x, y)) is mapped into a point in the normalized matrix (i.e., located in polar coordinates (r,θ)) as follows

$$
\begin{aligned}
x(r,\theta) &= (1-r)x_p(\theta) + r x_l(\theta) \\
y(r,\theta) &= (1-r)y_p(\theta) + r y_l(\theta)
\end{aligned}
\tag{1}
$$

where the value of r is in the interval $[0,1]$ and the value of θ is in the interval $[0,2\pi]$. $(x_p(\theta), y_p(\theta))$ and $(x_l(\theta), y_l(\theta))$ are the coordinates of the inner and outer boundaries in the direction of θ, respectively. It is worth mentioning that, in our work, the lower half of the iris ring is considered as the region of interest for feature extraction process. This region of interest is slightly affected by eyelids and eyelashes.

3.3. Feature Extraction

In this section, we describe the proposed algorithm for feature extraction. As previously mentioned, the textural information in the iris ring is stable and unique for each person. Hence, it may serve as a kind of living "passport" for each person. The feature vector is created by performing mathematical operations on the template and using the quantitative response as a feature. The accuracy of the matching process is determined by how well different patterns have been extracted and represented on the feature vector template. A good feature extraction method gives each individual's iris patterns its own distinct representation, allowing for accurate matching to be performed. Unlike most of the proposed techniques for feature extraction that are based on wavelet analysis, our proposed scheme accounts for any intensity changes when the images of the iris were acquired, eliminating any preliminary hardware used to adjust lighting as well as further software applications to reduce the effect of light intensity. The proposed algorithm is simply illustrated as follows:

- **Step 1.** Find the minimum and maximum gray values within a (1x15) sliding window centered at each point in the normalized region of interest.
- **Step 2.** Calculate the binary threshold for each point in the region of interest by finding the mid-point between the minimum and maximum values found in Step 1.
- **Step 3.** If the point value is greater than its binary threshold, the point is set to "1"; otherwise, it is set to "0".

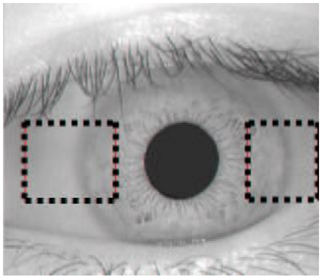

(a) 3-o'clock and 9-o'clock regions

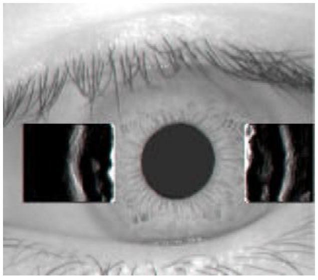

(b) The result of applying 9x9 median filter and then east and west compass kernels over 3- and 9- o'clock sides, respectively

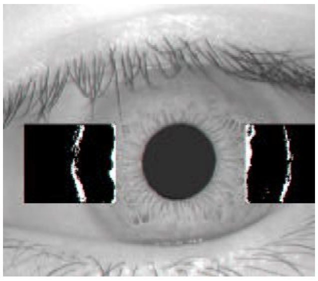

(c) The result of converting the search regions to binary images

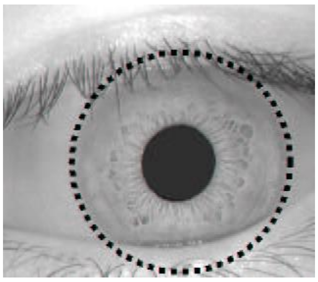

(d) The result of applying the circular Hough transform to find the outer boundary

Figure 4. Steps for finding the outer boundary of the iris in image 027-2-1 from CASIA database [12]

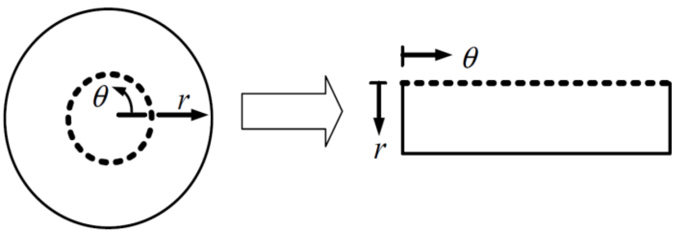

Figure 5. Daugman's mapping method for iris normalization

3.4. Matching

The Hamming distance (HD) technique was chosen as the matching method because the feature vectors created were binary, thus being ideal for this technique. The Hamming distance finds the number of corresponding bits that differ between two biometric templates. This is known as the dissimilarity between templates. The matching process allows us to decide whether the two compared irises belong to the same person or not. The Hamming distance between the binary templates A and B is defined as follows:

$$HD = \frac{1}{M} \sum_{j=1}^{M} A_j \oplus B_j \qquad (2)$$

where M is the number of bits in one of the compared templates and $\oplus$ is the XOR operation. Small HD means that the two templates are similar to each other. Assuming that there may be a possibility of rotation of the iris pattern during image acquisition, eight circularly rotated templates are first constructed for the image to be compared with the database. This is done by shifting the template columns four times to the right and four times to the left. These shifted templates, along with the original input template, give a total of nine templates to be used in the comparison. The smallest resulting Hamming distance is considered as the final matching ratio for the input.

It is noteworthy to mention that to tangibly speed up the calculation process of the Hamming distance, the XOR operation should be performed with an optimization technique in C/C++ [13]. Accordingly, calculating the Hamming distance using XOR operator allows the proposed scheme to be used in a large-scale identification system.

4. Performance Evaluation

To evaluate the performance of our scheme, we compare it with other closely connected schemes found in [2, 5, 20, 21, 24–27, 31–34, 36]. Experiments are conducted on CASIA iris database [12] which includes 756 eye images from 108 persons. Our code is written and implemented using the MATLAB program running on AMD Turion(tm) II Dual-Core Mobile M500 2.20 GHz.

4.1. The performance of Iris Segmentation

We use the Hough transform for iris segmentation. As explained in Section 3.1, we apply the Hough transform within a certain regions (i.e., 3-o'clock and 9-o'clock regions) in order to mitigate the main issue of the Hough transform (in online applications), which is the high computational time. Table 1 shows that the proposed iris segmentation method achieves a high correct segmentation rate with a computational time lower than that in [31] and [26]. In [31] and [26], to locate the iris region, several image processing techniques (e.g., edge detection, circular and linear Hough transform, polynomial fitting, and thresholding) were applied over the entire iris image.

Table 1. Comparison of the performance of different iris segmentation methods

Method	Correct segmentation rate	Average segmentation time for one iris (msec)
Masek [26]	83%	15670.3
Al-Zubi [31]	99%	994.3
Proposed	99%	719.4

4.2. The performance of Feature Extraction

A biometric system can run in two different modes: identification or verification. In the identification case, the system is trained with the patterns of several people. For each person, a biometric template is created. The input pattern is matched against every known template, yielding a matching ratio (i.e., Hamming distance) which describes the similarity between the pattern and template. The pattern with the highest matching ratio (i.e., smallest Hamming distance) is assigned to that person. In the verification case, the pattern that is verified is only compared with the templates in the class corresponding to that individual. Therefore, there are two classes of iris comparisons:

- Intra-class Comparisons: Comparison of an iris image with other images registered to the same person. This is referred to as a verification process.
- Inter-class Comparisons: Comparison of an iris image with all iris images to find to whom it belongs to (if they match any person in the database or not). This is referred to as an identification process.

Two interesting performance metrics were employed to evaluate the performance of our proposed method, namely, the false acceptance rate (FAR) and false rejection rate (FRR). The FAR, or type II error, measures the probability that an unauthorized person is identified by the system as an authorized person. FAR can be calculated as follows:

$$FAR = \frac{\int_0^T P_{inter}(x)dx}{\int_0^1 P_{inter}(x)dx} \qquad (3)$$

where $P_{inter}(x)$ is the distribution of the interclass comparisons and T is the threshold between the inter- and intra-class distributions shown in Fig. 6. This threshold is determined experimentally to minimize FAR and FRR. For our work, the threshold found to give the lowest FRR and FAR values is 0.41, see Table 2.

The FRR, or type I error, measures the probability that the system fails to recognize an authorized person and rejects that person as an impostor. FRR can be calculated as follows:

$$FRR = \frac{\int_T^1 P_{intra}(x)dx}{\int_0^1 P_{intra}(x)dx} \qquad (4)$$

where $P_{intra}(x)$ is the distribution of the intra-class comparisons.

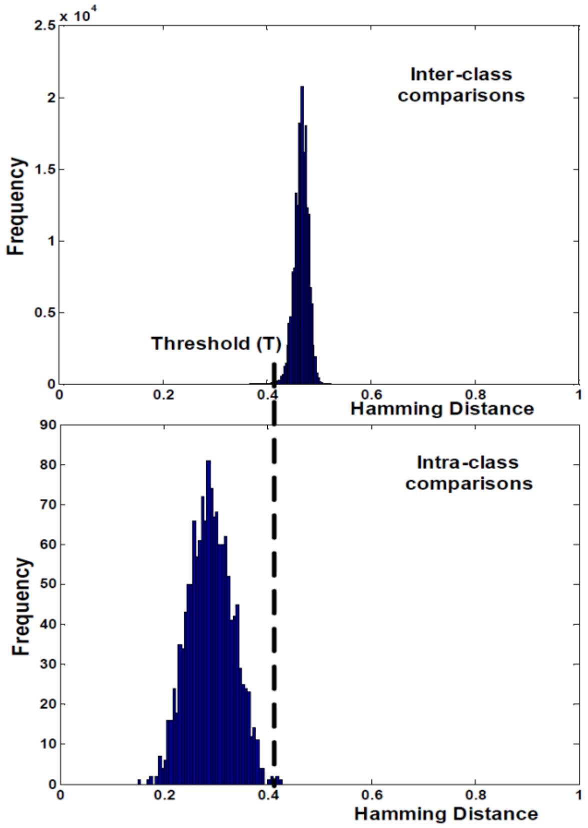

Figure 6. Inter-class and intra-class distributions

Table 2. FAR and FRR at different thresholds

Threshold	FRR(%)	FAR(%)
0.43	0.000	0.639
0.42	0.044	0.200
0.41	**0.176**	**0.078**
0.40	0.309	0.029
0.39	0.485	0.011
0.38	0.926	0.004
0.37	1.896	0.000

In Fig. 7, we plot FRR against FAR (i.e., the receiver operating characteristic (ROC) curve) to show the overall performance of our scheme with respect to that of other proposed schemes [2], [31], [25], [6], [24]. The figure shows that our proposed scheme achieves a high performance. Moreover, our scheme is unlike the compared schemes that are based on wavelet analysis, which needs a huge processing time to be performed as well as the parameters of the wavelet analysis were selected and fixed in advance which could not properly work for possible changes in the quality of the captured iris image (owing to different image capturing conditions such as capturing distance, light intensity, etc.). Moreover, the method in [6] can be applied for personal verification process only, but our proposed scheme is applicable for verification and identification processes.

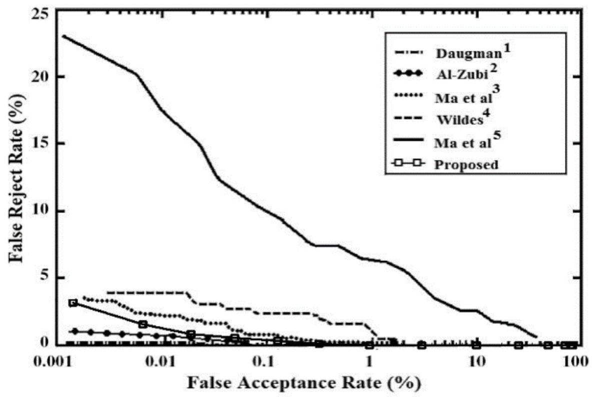

Figure 7. Comparison of ROC curves for several schemes (1- [2], 2- [31], 3- [25], 4- [6], 5- [24])

In addition to FAR and FRR performance metrics, we employed the correct recognition rate (CRR) which can be defined as the ratio of the number of input images being correctly recognized to the total number of input images entered into the system. Table 3 compares the results of our iris recognition system with other methods (the results of these methods are also reported in [36]). It shows that our proposed scheme achieves a high CRR. Moreover, all the compared methods are based on wavelet analysis which has some problems as we previously discussed.

Table 3. Recognition rate for different iris-recognition schemes

Method	Feature Extraction	CRR (%)
Daugman (2001) [20]	2-D Gabor filter	100%
Narote et al (2007) [32]	Dual tree complex wavelet transform	99.20%
Poursaberi (2007) [33]	Four-level wavelet transform	97.22%
Xiaofu (2008) [34]	Two dimensional complex wavelet transform	98.15%
Abdullah et al (2011) [36]	Haar wavelet decomposition	99.0%
Proposed	Simple local binary quantization	99.34%

7. Conclusion

In this paper, we have introduced efficient methods for iris segmentation and feature extraction of human iris patterns. To get an accurate and fast segmentation, the scheme exploits the 3-o'clock and 9-o'clock sides of the iris to find the outer boundary. These regions are usually the most clear parts of the outer boundary (slightly affected by eyelids and eyelashes). For feature extraction, the lower half of the iris region was selected as a region of interest. This region is usually the most clear and visible region in the iris (i.e., slightly interfered by eyelashes and eyelids). From this region of interest, the iris features were extracted by using a proposed technique that is based on local binary quantization. This technique eliminates the effect of light intensity variations on the images acquired for iris recognition. Through experimentation, it was found that our method achieves high performance in terms of speed and accuracy. This validates that our iris segmentation and feature extraction steps do perform iris recognition accurately and that our analysis and understanding are rational and practical.

References

[1] **L. Flom**. Iris recognition system. *Patent No. 4641349*, 1987.

[2] **J. Daugman**. Biometric personal identification system based on iris analysis. *Patent No. 5291560*, 1994.

[3] **J. Daugman**. How iris recognition works. In: *Proceedings of the International Conference on Image Processing (ICIP), Rochester, New York, USA*, 2002, pp. 1-36.

[4] **J. Daugman.** How iris recognition works. *Patent No. 5291560*, 1994.

[5] **R. Wildes, J. Asmuth, K. Hanna, S. Hsu, R. Kolczynski, J. Matey, S. McBride**. Automated, non-invasive iris recognition system and method. *Patent No. 5,572,596*, 1996.

[6] **R. Wildes**. Iris recognition: an emerging biometric technology. In: *Proceedings of the IEEE*, September 1997, Vol. 85, pp. 1348-1363.

[7] **A. Jain, A. Ross, S. Prabhakar**. An introduction to biometric recognition. *IEEE Transactions on Circuits and Systems for Video Technology*, January 2004, Vol. 14, No. 1, 4-20.

[8] **M. Kamada**. Iris authentication apparatus. *Patent No. 6785406*, 2004.

[9] **J. Ali and A. Hassanien**. An iris recognition system to enhance e-security environment based on wavelet theory. In: *On Wavelet Theory, AMO - Advanced Modeling and Optimization*, 2003, pp. 93-104.

[10] **S. Lim, K. Lee, O. Byeon, T. Kim**. Efficient iris recognition through improvement of feature vector and classifier. *ETRI Journal*, June 2001, Vol. 23, No. 2, 61-70.

[11] **M. Matsushita**. Iris identification system and iris identification method. *Patent No. 5,901,238*, 1999.

[12] CASIA iris image database. http://biometrics.idealtest.org/index.jsp, 2003.

[13] **W. Chen, J. Lee, W. Han, C. Shih, K. Chang**. Iris recognition based on bidimensional empirical mode decomposition and fractal dimension. *Information Sciences*, 2013, Vol. 221, No. 2, 439-451.

[14] **H. Wu**. Optimal gabor filters for high speed face identification. In: *Proceedings of the International Conference on Pattern Recognition (ICPR), Quebec, Canada*, 2002, pp. 107-110.

[15] **P. Lipinski and M. Yatsymirskyy.** New algorithm for calculating wavelet transforms. *Journal of Systemics, Cybernetics, and Informatics*, March 2009, Vol. 7, No. 2, 46-50.

[16] **G. Amayeh, A. Tavakkoli, G. Bebis**. Accurate and efficient computation of Gabor features in realtime applications. In: *Proceedings of the 5th International Symposium on Advances in Visual Computing: Part I (ISVC), Las Vegas, Nevada, USA*, 2009, pp. 243-252.

[17] **F. Han, L. Guan, Z. Wang**. A new algorithm for generalized wavelet transform. *Advances in Neural Networks*, 2010, LNCS Vol. 6063, 311-318.

[18] **J. Daugman**. Probing the uniqueness and randomness of iriscodes: results from 200 billion iris pair comparisons. In: *Proceedings of the IEEE*, November 2006, Vol. 94, No. 11, pp. 1927-1935.

[19] **J. Daugman**. New methods in iris recognition. *IEEE Transactions on Systems, Man, and Cybernetics, Part B: Cybernetics*, October 2007, Vol. 37, No. 5, 1167-1175.

[20] **J. Daugman**. Statistical richness of visual phase information: Update on recognizing persons by iris patterns. *International Journal of Computer Vision*, October 2001, Vol. 45, No. 1, 25-38.

[21] **W. Boles, B. Boashash**. A human identification technique using images of the iris and wavelet transform. *IEEE Transactions on Signal Processing*, April 1998, Vol. 46, No. 1, 1185-1188.

[22] **Y. Zhu, T. Tan, Y. Wang**. Biometric personal identification based on iris patterns. In: *Proceedings of the International Conference on Pattern Recognition (ICPR), Barcelona, Spain*, 2000, pp. 805-808.

[23] **C. Tisse, L. Martin, L. Torres, M. Robert**. Person identification technique using human iris recognition. In: *Proceedings of the International Conference on Vision Interface (ICVI), Calgary, Canada*, pages 2002, pp. 294-299.

[24] **L. Ma, Y. Wang, T. Tan**. Iris recognition based on multichannel gabor filtering. In: *Proceedings of the International Conference on Asian Conference on Computer Vision (ACCV), Melbourne, Victoria, Australia*, 2002, pp. 279-283.

[25] **L. Ma, Y. Wang, T. Tan**. Iris recognition using circular symmetric filters. In *Proceedings of the International Conference on Pattern Recognition (ICPR), Quebec, Canada*, 2002, pp. 414-417.

[26] **L. Masek, P. Kovesi**. Matlab source code for a biometric identification system based on iris patterns. *School of Computer Science and Software Engineering, University of Western Australia, Perth, Australia*, 2003.

[27] **L. Ma, T. Tan, Y. Wang, D. Zhang**. Personal identification based on iris texture analysis. *IEEE Transactions on Pattern Analysis and Machine Intelligence*, 2003, Vol. 25, No. 12, 1519-1533.

[28] **S. Noh, K. Bae, K. Park, J. Kim**. A new iris recognition method using independent component analysis. *IEICE-Transactions on Information and Systems*, 2005, Vol. E88-D, No. 11, 2573-2581.

[29] **D. Monro, S. Rakshit, D. Zhang**. DCT-based iris recognition. *IEEE Transactions on Pattern Analysis and Machine Intelligence*, April 2007, Vol. 29, No. 4, 586-595.

[30] **H. Proenca, L. Alexandre.** Toward noncooperative iris recognition: a classification approach using multiple signatures. *IEEE Transactions on Pattern Analysis and Machine Intelligence*, 2007, Vol. 29, No. 4, 607-612.

[31] **R. Al-Zubi, D. Abu Al-Nadi.** Automated personal identification system based on human iris analysis. *Pattern Analysis and Applications (PAA)*, May 2007, Vol. 10, No. 2,147-164.

[32] **S. Narote, A. Narote, L. Waghmare, M. Kokare, A. Gaikwad**. An iris recognition based on dual tree complex wavelet transform. In: *Proceedings of TENCON 2007 - 2007 IEEE Region 10 Conference*, October 2007, pp. 1-4.

[33] **A. Poursaberi, B. Araabi**. Iris recognition for partially occluded images: Methodology and sensitivity analysis. *EURASIP Journal on Advances in Signal Processing*, 2007, Vol. 2007, 1-12.

[34] **H. Xiaofu, S. Pengfei**. Extraction of complex wavelet features for iris recognition. In *Proceedings of the International Conference on Pattern Recognition (ICPR), Tampa, Florida, USA*, December 2008, pp. 1-4.

[35] **C. Tsai, J. Taur, C. Tao**. Iris recognition using Gabor filters and the fractal dimension. *Journal of Information Science and Engineering*, 2009, Vol. 25, No. 2, 633-648.

[36] **M. Abdullah, F. Al-Dulaimi, W. Al-Nuaimy, A. Al-Ataby**. Efficient small template iris recognition system using wavelet transform. *International Journal of Biometric and Bioinformatics*, 2011, Vol. 5, No. 1, 16-27.

Received September 2013.